



# Structural characterisation of the giant organometallic platinum cluster $\text{Pt}_{309}(\text{phen}^*)_{36}\text{O}_{30}$ using EXAFS<sup>1</sup>

R.E. Benfield<sup>a,\*</sup>, A. Filipponi<sup>a,b</sup>, N. Morgante<sup>a,c</sup>, G. Schmid<sup>d</sup>

<sup>a</sup> Centre for Materials Research, School of Physical Sciences, University of Kent, Canterbury CT2 7NR, UK

<sup>b</sup> ESRF, BP 220, F38043 Grenoble, France

<sup>c</sup> Dipartimento di Scienza dei Materiali, Università di Milano, Via Emanuelli 15, I-20126 Milan, Italy

<sup>d</sup> Institut für Anorganische Chemie, Universität GH Essen, Universitätsstrasse 5-7, D-45117 Essen, Germany

Received 15 May 1998

## Abstract

The structure of the high-nuclearity organometallic platinum cluster material  $\text{Pt}_{309}(\text{phen}^*)_{36}\text{O}_{30}$  has been investigated by X-ray absorption spectroscopy. Analysis of Pt L<sub>3</sub>-edge EXAFS data, using platinum foil as a reference, shows that the platinum clusters have cubic close packed geometry. A slight contraction of the Pt–Pt bond length from the bulk was observed. XANES analysis shows that the platinum atoms in the clusters have a low mean oxidation state, very close to that in metallic platinum. © 1999 Elsevier Science S.A. All rights reserved.

**Keywords:** Platinum; Clusters; EXAFS; Lattice contraction; XANES

## 1. Introduction

Organometallic cluster compounds have become one of the most intensely studied fields of chemistry. Clusters containing several tens of atoms have been synthesised and characterised [1,2]. Transition metal carbonyl clusters form the most extensive series of these compounds; there are also many phosphine halide clusters of gold. The structural parallels between these molecular cluster compounds and small particles of metal have long been recognised [1,3]. The arrangements of ligands on the cluster surfaces have also been studied [4].

The spectroscopic and physical properties of these metal cluster compounds have become of intense interest. Appropriate measurements can characterise the way in which the well-separated energy levels of a small

metal atom cluster develop into an effective band structure in larger clusters [5]. An important question is whether there is a smooth transition with increasing cluster size from ‘molecular’ towards ‘bulk metallic’ behaviour, or whether the transition is more complex, with an intermediate ‘metametallic’ region showing unusual properties different from either limit and displaying quantum-size effects [6–8].

It has also been recognised that there are many different criteria for ‘metallic’ behaviour, and that these may be attained at greatly different nuclearities. For example, in gold clusters of 55 atoms, the ‘interband’ 5d → 6s, 6p electronic transition in the UV-visible is quite similar to that of colloidal gold; but in the same clusters, the plasma resonance absorption of delocalised 6s conduction electrons, characteristic of gold colloids, is almost entirely absent [9,10].

Recently, several types of non-crystalline high-nuclearity metal clusters have been prepared. These materials, stabilised by ligands which may be monodentate, bidentate, or act as bridges between clusters, represent

\* Corresponding author. Tel.: +44 1227 823558; fax: +44 1227 827558; e-mail R.E.Benfield@ukc.ac.uk

<sup>1</sup> Dedicated to Professor Brian Johnson on the occasion of his 60th birthday, in recognition of his outstanding contributions to organometallic, inorganic and cluster chemistry.

an interface between molecular clusters and colloids [11–14].

In interpreting the physical and spectroscopic properties of these high-nuclearity organometallic materials, structural characterisation is important. However, they cannot be obtained in a form suitable for X-ray crystallographic study. Their structures and interatomic distances must be determined by methods appropriate for amorphous materials, such as EXAFS [15].

There are two key structural issues in these giant organometallic clusters. Firstly, is their geometric structure cubic close-packed, or do they adopt some other geometry such as icosahedral? Secondly, are the metal–metal distances in the clusters the same as in the corresponding bulk metals, or is there a contraction reflecting a changed bonding environment and the effect of a high surface:bulk ratio?

EXAFS can answer both these questions by probing the local environment of the metal atoms in a cluster. At the same time, the X-ray absorption spectrum used for the EXAFS analysis can give information from its near-edge region (XANES) on the effective oxidation state of the metal atoms in the cluster.

We have previously reported the results of EXAFS studies on organometallic gold and palladium clusters. EXAFS confirmed the crystallographically known icosahedral-based structure of a molecular  $\text{Au}_{11}$  cluster by resolving the 0.2 Å splitting between the radial and tangential nearest-neighbour interatomic distances, which differ in an icosahedron by about 5%. No such splitting could be resolved in  $\text{Au}_{55}(\text{PPh}_3)_{12}\text{Cl}_6$ , which was therefore concluded to have a cubic close-packed cluster structure [16]. The Au–Au nearest neighbour distance in  $\text{Au}_{55}(\text{PPh}_3)_{12}\text{Cl}_6$  was found to be about 4% contracted from that in bulk gold [16,17]. The palladium cluster material  $\text{Pd}_{561}(\text{phen})_{36}\text{O}_{200}$ , was also found to be cubic close-packed, but in this case no significant contraction of the metal–metal distance was observed [16,18]. Consistent with this, differential scanning calorimetry measurements of the thermal decomposition of the clusters have shown that the Au–Au bonds in  $\text{Au}_{55}(\text{PPh}_3)_{12}\text{Cl}_6$  are substantially stronger than in bulk gold [19], but the Pd–Pd bonds in  $\text{Pd}_{561}(\text{phen})_{36}\text{O}_{200}$  are slightly weaker than in bulk palladium [20]. This parallels the behaviour of the corresponding metals in the absence of ligands. Lattice contractions are consistently found in small gold particles [21]. For small palladium particles, most experimental measurements have shown lattice expansions from the bulk [22], although lattice contractions have also been reported [23].

We now report the results of Pt  $L_3$ -edge EXAFS analysis of the cluster material of ideal formulation  $\text{Pt}_{309}(\text{phen}^*)_{36}\text{O}_{30}$  (where phen\* represents a sulphonated phenanthroline ligand, which gives the cluster high aqueous solubility). High-resolution elec-

tron microscopy and X-ray powder diffraction have previously shown that  $\text{Pt}_{309}(\text{phen}^*)_{36}\text{O}_{30}$  contains nearly monodisperse platinum atom clusters of diameter 17.5 Å, which have a cubic close-packed structure of cuboctahedral geometry with the Pt–Pt distance very close to that in the bulk metal [24]. Mössbauer studies, using a novel method in which platinum atoms are transmuted to  $^{197}\text{Au}$  by neutron irradiation, have shown that the metal atoms in the inner core of the  $\text{Pt}_{309}$  cluster have substantially metallic character [25]. NMR studies on the  $^{195}\text{Pt}$  nucleus have shown a Knight-shifted peak from the core atoms, for which metallic behaviour was inferred [26] from the temperature-dependence of the relaxation time  $T_1$ .

## 2. Experimental

$\text{Pt}_{309}(\text{phen}^*)_{36}\text{O}_{30}$  was prepared by controlled reduction of Pt(II) acetate with hydrogen in the presence of protecting ligands, followed by oxidation with oxygen [24]. Finely ground samples were diluted with boron nitride powder and pressed into pellets for EXAFS measurements in transmission mode. A 25-micron thick platinum foil (Goodfellow Metals) was used as a reference sample. X-ray absorption spectra were collected at the SRS facility (Daresbury Laboratory, UK), on beamline 7.1. Data were collected at 80, 190, and 300 K, for evaluation of the relative importance of static and thermal disorder. An excellent signal to noise ratio up to about  $k = 18 \text{ \AA}^{-1}$  was obtained (Fig. 1).

The Pt  $L_2$  X-ray absorption edge of the cluster was also recorded for XANES analysis using platinum foil (Goodfellow) and  $\text{K}_2\text{PtCl}_4$  (Johnson Matthey) as reference materials.

## 3. Data analysis

EXAFS data analysis was performed using both calculated and experimental phase-shifts and backscattering amplitudes ( $\delta(k)$  and  $A(k)$ , respectively). Two analysis program packages were employed, namely GNXAS [27] and WINXAS [28]. GNXAS allows a calculation of phase shifts employing a complex Hedin-Lundqvist potential. WINXAS allows analysis using experimental  $\delta(k)$  and  $A(k)$ , which are extracted performing a fit on the EXAFS signal of the reference compound, extracting reliable information from the frequency of the EXAFS signal, rather than its amplitude. Full account was taken of both curved-wave and multiple-scattering effects. The first neighbour metal–metal distribution was modelled by a gamma-like [29] distribution depending on four parameters: coordination number  $N$ , average distance  $R$ , variance  $\sigma^2$  and asymmetry  $\beta$ . This model takes account of possible

asymmetry effects in the interatomic radial distribution, simulating both positively and negatively skewed distributions passing continuously through the Gaussian limit  $\beta = 0$ . The statistical error evaluation accounted for the correlations between radial distances and absorption energy threshold, and between pseudo Debye–Waller factors and coordination numbers.

Refinements were carried out using  $k^3$  and  $k^2$  weighting. The refined parameters were virtually identical in both cases. Final fits are reported using  $k^2$  weighting, which gave a more even amplitude to the weighted EXAFS oscillations up to high  $k$ -values (see Fig. 1). Phase-shifts calculated by GNXAS have shown to be somewhat inaccurate in the low- $k$  region. Thus, final fitting was performed with a relatively high low limit for the energy range (ca.  $4 \text{ \AA}^{-1}$ ).

XANES analysis was carried out using the ' $L_3 - kL_2$ ' method reported by Moraweck et al. [30]. The  $L_3$  and  $L_2$  spectra were subtracted after normalisation of the step to unity. Energy calibration was performed minimising the difference of the normalised spectra in a

region ranging from 40 to 100 eV above the edge. Areas were computed using the trapezoidal rule.

#### 4. EXAFS refinements

Results of the EXAFS structural refinements for Pt foil and  $\text{Pt}_{309}(\text{phen}^*)_{36}\text{O}_{30}$  are shown in Table 1. The EXAFS signal of bulk platinum was successfully fitted up to the fourth shell. The refined parameters agree well with crystallographic data.

For the  $\text{Pt}_{309}$  cluster, the data collected at 190 and 300 K showed a lower signal to noise ratio than those from 80 K, because of greater dynamic disorder. They could be fitted only over a relatively limited  $k$ -region, with a consequent loss of resolution in real space, so that only the first shell could be satisfactorily fitted in these cases.

Data collected at 80 K are therefore to be considered the main source of structural information for the  $\text{Pt}_{309}$  clusters. Four shells of platinum atoms were success-

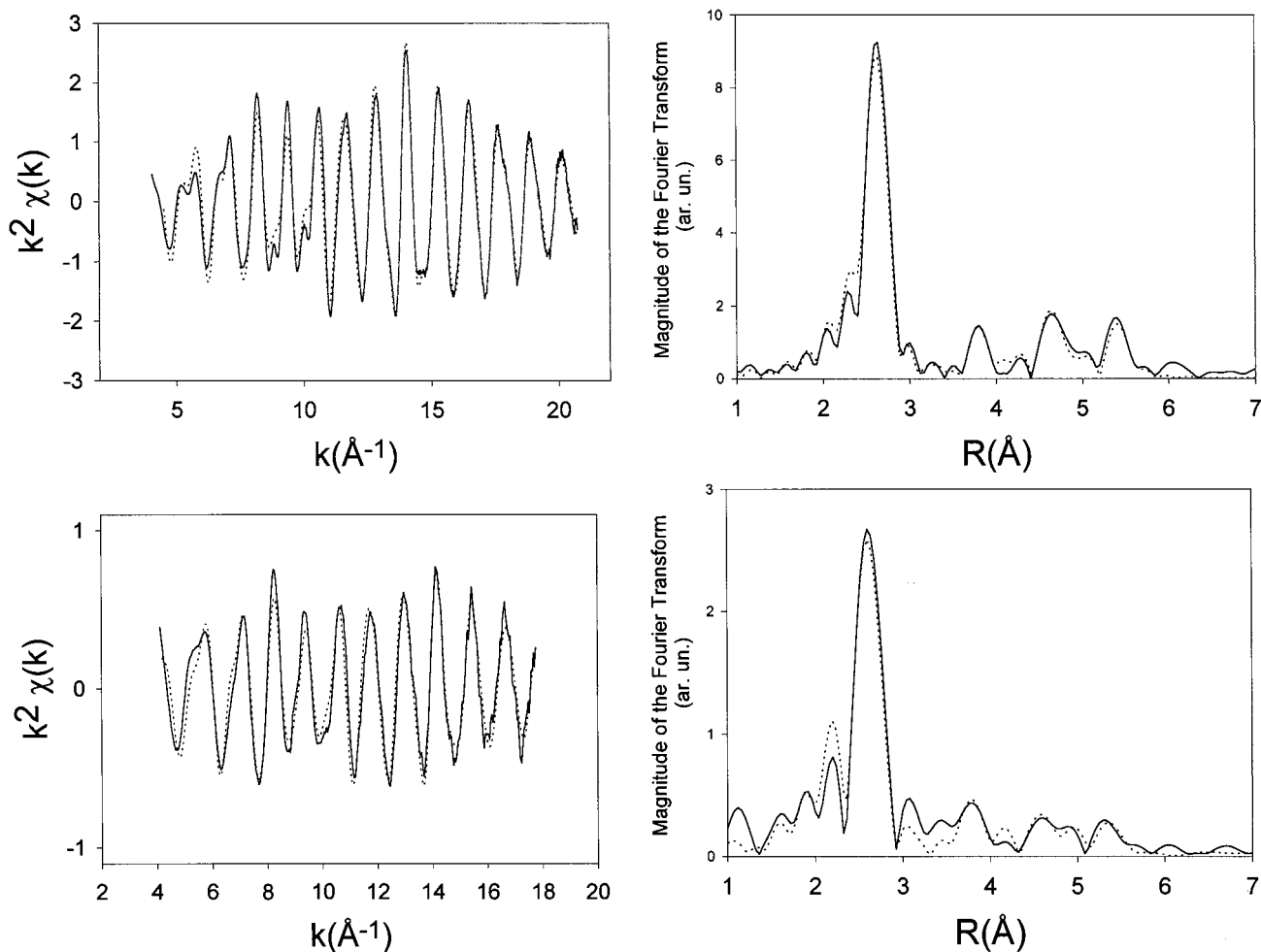


Fig. 1. Pt  $L_3$ -edge EXAFS spectra (after background subtraction,  $k^2$ -weighted) and Fourier transforms for (left) Pt foil and (right)  $\text{Pt}_{309}(\text{phen}^*)_{36}\text{O}_{30}$ . The solid lines are the experimental data and the dotted lines are the best fits.

Table 1  
Summary of structural results of Pt L<sub>3</sub>-edge EXAFS refinements: Pt–Pt distances for Pt foil and Pt<sub>309</sub> cluster

		Pt foil (80 K)	Pt <sub>309</sub> (80 K)	Pt <sub>309</sub> (190 K)	Pt <sub>309</sub> (300 K)
1st shell	R (Å)	2.767 ± 0.003	2.74 ± 0.01	2.74 ± 0.02	2.74 ± 0.03
	σ <sup>2</sup> (10 <sup>-3</sup> Å <sup>2</sup> )	2.5 ± 0.5	4.0 ± 1	7.0 ± 1	10.0 ± 1
	N	12.0 ± 1	7.0 ± 3	8.0 ± 3	8.0 ± 3
2nd shell	R (Å)	3.91 ± 0.01	3.87 ± 0.02		
	σ <sup>2</sup> (10 <sup>-3</sup> Å <sup>2</sup> )	5.0 ± 1	7.0 ± 3		
	N	6.0 ± 0.5	2.0 ± 1		
3rd shell	R (Å)	4.79 ± 0.01	4.75 ± 0.02		
	σ <sup>2</sup> (10 <sup>-3</sup> Å <sup>2</sup> )	5.0 ± 1	7.0 ± 3		
	N	24.0 ± 2	7.0 ± 3		
4th shell	R (Å)	5.53 ± 0.01	5.46 ± 0.02		
	σ <sup>2</sup> (10 <sup>-3</sup> Å <sup>2</sup> )	5.0 ± 1	7.0 ± 3		
	N	12.0 ± 1	3.0 ± 2		

fully fitted, the fourth shell being emphasised by multiple scattering effects due to a three-body configuration with Pt atoms in a co-linear arrangement.

The first shell Pt–Pt distance at 80 K showed a Gaussian profile, with no significant asymmetry or splitting. Distances corresponding to the second and third shells were found to be almost exactly equal to  $\sqrt{2}$  and  $\sqrt{3}$  times the distance of the nearest neighbour, respectively. Both findings show that the Pt<sub>309</sub> clusters have a bulk-like fcc structure, as previously suggested [24].

A very slight contraction of the average Pt–Pt distance compared to the bulk value, amounting to about 1% and just significant within our experimental resolution, was observed for the cluster sample at 80 K. This contraction for the ligand-stabilised Pt<sub>309</sub> clusters can be compared to the 0.4% lattice contraction previously found by EXAFS for polymer-protected platinum colloids of 26 Å diameter [31], and to the 4.3% contraction found for helium-coated platinum particles of 14 Å diameter [32].

Errors can arise in the EXAFS bond length analysis of small metal particles if the anharmonicity of their atomic motions is not taken into account, leading to the possibility that observed lattice contractions are artefacts of the refinement procedure [33,34]. This is not the case in our analysis, which has taken full account of the possibility of asymmetric bond length distributions that would arise from anharmonic atomic motions. Asymmetry (measured by a skewing factor to the Gaussian factor of the EXAFS function) was found to be negligible in Pt<sub>309</sub>(phen\*)<sub>36</sub>O<sub>30</sub> at 80 K. It increased with temperature, and at 300 K was high enough to lead to an apparent distance contraction of ca. 0.03 Å when not accounted for.

Unfortunately, the Pt–Pt distance in Pt<sub>309</sub>(phen\*)<sub>36</sub>O<sub>30</sub> cannot be correlated with the strength of the Pt–Pt

bonding, as was achieved in previous work on gold and palladium clusters, because thermal decomposition of this cluster does not show a clear calorimetric signal necessary for the calculation of its decomposition enthalpy [20].

The values of the variance  $\sigma^2$  in the Pt–Pt bond length distributions at 80 K (Table 1) show that the clusters are affected by a slight increase in structural disorder from bulk platinum. This is in line with expectations, and with our previous findings for palladium clusters [18]. The variance for the clusters showed a satisfactory temperature-dependence, further confirming the accuracy of our refinements and suggesting that the thermal behaviour of these clusters resembles that of bulk platinum.

The coordination numbers *N* of the platinum shells in the cluster were allowed to refine freely, to avoid placing artificial constraints on the refinements. The resulting values (Table 1) are substantially lower than for bulk platinum, as expected from the presence of a high proportion of surface atoms in the clusters. However, the values are lower than expected (ideally 9.63 for the mean nearest-neighbour coordination number in a cuboctahedral cluster of 309 atoms) [35]. A similar effect has often been observed in previous EXAFS studies of metal clusters and colloids [18,31], although our careful treatment of asymmetry and correlation effects should have avoided any systematic error in the coordination numbers [36]. The resolution of long-range platinum distances up to the fourth shell at 80 K confirms that these low coordination numbers cannot be explained by a smaller average cluster size. The most probable cause is the presence of a small amount of mononuclear platinum material arising from the synthetic procedure. A similar conclusion was reached in our previous study of palladium clusters [18].

The inclusion of an extra shell accounting for light atoms (nitrogen or oxygen) led to a small statistically significant improvement in the Pt L<sub>3</sub>-edge EXAFS refinement. A broad distribution function peaking at 2.10 Å resulted from the fit. However it is not clear whether this represents ligand atoms bound to platinum atoms on the surfaces of the clusters, a contribution from mononuclear platinum material, or the summation of both.

## 5. XANES analysis

X-ray absorption L-edges correspond to the excitation of an electron from a core 2p level to a vacant d-orbital. The intensity of these so-called 'white lines' gives a measure of the extent to which the d-orbitals are vacant, and can be correlated with the real oxidation state of the absorbing atom [37]. Specifically, the difference between Pt L<sub>3</sub> and L<sub>2</sub> spectra yields information on the density of unoccupied states in the 5d<sub>5/2</sub> band [30]. The 'L<sub>3</sub> - kL<sub>2</sub>' method employed here minimises problems associated with energy calibration, since it is based on the comparison between L<sub>3</sub> and L<sub>2</sub> spectra taken from the same sample.

Area values of the difference spectra (given as eV times the step) were found to be: Pt foil 6.9 ± 0.3; Pt<sub>309</sub> 6.7 ± 0.3; K<sub>2</sub>PtCl<sub>4</sub> 8.1 ± 0.3. The values for the Pt<sub>309</sub> cluster and platinum metal differ by less than the experimental error, showing a difference in 5d<sub>5/2</sub>-band occupancy of less than 5%. Any mononuclear platinum complexes present in the cluster sample must be expected to have a positive oxidation state. Therefore it can be clearly concluded that the platinum atoms in the clusters have a low mean oxidation state, very close to that in metallic platinum. This is fully consistent with the earlier evidence from Mössbauer [25] and NMR [26] spectroscopy that the platinum atoms in the Pt<sub>309</sub> cluster cores have substantially metallic character.

## 6. Discussion

A significant outcome of our EXAFS studies is that we have found substantially different degrees of lattice contraction in giant ligand-stabilised clusters of different metals: 4% in Au<sub>55</sub>(PPh<sub>3</sub>)<sub>12</sub>Cl<sub>6</sub>, 1% in Pt<sub>309</sub>(phen\*)<sub>36</sub>O<sub>30</sub>, and well under 1% in Pd<sub>561</sub>(phen)<sub>36</sub>O<sub>200</sub>. Re-refinement of the Au<sub>55</sub>(PPh<sub>3</sub>)<sub>12</sub>Cl<sub>6</sub> data using GNXAS has confirmed the earlier results, which were obtained using EXCURV. All these studies have now accounted in the same way for the possibility of asymmetric bond length distributions arising from anharmonic atomic motions in the clusters, so that the different bond length contractions cannot be artefacts of the refinement proce-

dure. This further confirms that the lattice contraction observed in Au<sub>55</sub>(PPh<sub>3</sub>)<sub>12</sub>Cl<sub>6</sub> is real.

It remains an open question whether the different degrees of contraction found for the gold, palladium and platinum clusters result from genuine differences in the electronic character of these three metals, or simply reflect the various cluster sizes we have been able to study. Recent density functional calculations on clusters of palladium and gold [38] have predicted bond length contractions for both metals, correlating directly with the mean nearest-neighbour coordination number [35], and therefore with cluster size.

Finally, we point out that this EXAFS structural characterisation of Pt<sub>309</sub>(phen\*)<sub>36</sub>O<sub>30</sub> is relevant to the interpretation of studies of the mechanism of platinum-catalysed hydrosilation reactions. There is substantial evidence for the involvement of colloidal platinum particles in these reactions [39,40]. However, EXAFS studies of species isolated from the reaction have not been able to resolve outer-neighbour Pt–Pt distances [41]. The successful resolution of four Pt coordination shells at 80 K in Pt<sub>309</sub>(phen\*)<sub>36</sub>O<sub>30</sub> may place an upper limit on the size of the clusters involved in the hydrosilation catalysis.

## Acknowledgements

For financial support, we thank the Royal Society, the EPSRC, the EU SCIENCE Plan and the EU HCM and TMR Programmes.

## References

- [1] B.F.G. Johnson, *Transition Metal Clusters*, Wiley, Chichester, 1980.
- [2] G. Schmid, *Clusters and Colloids: from Theory to Applications*, VCH, Weinheim, 1994.
- [3] P. Chini, *Pure Appl. Chem.* 200 (1980) 37.
- [4] R.E. Benfield, B.F.G. Johnson, *J. Chem. Soc. Dalton Trans.* (1980) 1743.
- [5] D.M.P. Mingos, *Chem. Soc. Rev.* 15 (1986) 31.
- [6] R.E. Benfield, *J. Phys. Chem.* 91 (1987) 2712.
- [7] S.R. Drake, P.P. Edwards, B.F.G. Johnson, J. Lewis, D. Obertelli, N.C. Pyper, *J. Chem. Soc. Chem. Commun.* (1987) 1190.
- [8] L.J. de Jongh (Ed.), *Physics and Chemistry of Metal Cluster Compounds*, Kluwer, Dordrecht, 1994.
- [9] R.E. Benfield, A.P. Maydwell, J.M. van Ruitenbeek, D.A. van Leeuwen, *Z. Phys D26* (1993) S4.
- [10] R.E. Benfield, *Physics and Chemistry of Metal Cluster Compounds*, Kluwer, Dordrecht, 1994, pp. 249.
- [11] G. Schmid, *Struct. Bonding* 62 (1985) 51.
- [12] G. Schmid, *Chem. Rev.* 92 (1992) 1709.
- [13] R.L. Whetten, J.T. Khoury, M.M. Alvarez, et al., *Adv. Mater.* 8 (1996) 428.
- [14] M. Brust, D. Bethell, D.J. Schiffrin, C.J. Kiely, *Adv. Mater.* 7 (1995) 795.

- [15] D.C. Koningsberger, R. Prins (Eds.), X-ray Absorption: Principles, Applications and Techniques of EXAFS, SEXAFS and XANES, Wiley, Chichester, 1988.
- [16] P.D. Cluskey, R.J. Newport, R.E. Benfield, S.J. Gurman, G. Schmid, *Z. Phys D26* (1993) S8.
- [17] M.C. Fairbanks, R.E. Benfield, R.J. Newport, G. Schmid, *Solid State Commun.* 73 (1990) 431.
- [18] R.E. Benfield, A. Filipponi, D.T. Bowron, R.J. Newport, S.J. Gurman, G. Schmid, *Physica B* 208–209 (1995) 671.
- [19] R.E. Benfield, J.A. Creighton, D.G. Eadon, G. Schmid, *Z. Phys D12* (1989) 533.
- [20] G. Schmid, H. Hess, *Z. Anorg. Allg. Chem.* 621 (1995) 1147.
- [21] C. Solliard, M. Flueli, *Surf. Sci.* 156 (1985) 487.
- [22] C. Goyhenex, C.R. Henry, J. Urban, *Philos. Mag.* A69 (1994) 1073.
- [23] R. Lamber, S. Wetjen, N.I. Jaeger, *Phys. Rev. B* 51 (1995) 10968.
- [24] G. Schmid, B. Morun, J.O. Malm, *Angew. Chem. Intl. Edn.* 28 (1989) 779.
- [25] F.M. Mulder, T.A. Stegink, R.C. Thiel, L.J. de Jongh, G. Schmid, *Nature* 367 (1994) 716.
- [26] D. van der Putten, H.B. Brom, J. Witteveen, L.J. de Jongh, G. Schmid, *Z. Phys. D* 26 (1993) 21.
- [27] (a) A. Filipponi, A. Di Cicco, C.R. Natoli, *Phys. Rev. B*, 52 (1995) 15122. (b) A. Filipponi, A. Di Cicco, *Phys. Rev. B*, 52 (1995) 15135.
- [28] T. Ressler, *J. Phys. IV (Paris) (Suppl. C2)* 7 (1997) 269.
- [29] P. D'Angelo, A. Di Nola, A. Filipponi, N.V. Pavel, D. Roccatano, *J. Chem. Phys.* 100 (1994) 985.
- [30] B. Moraweck, A.J. Renouprez, E.K. Hill, R. Baudoing-Savois, *J. Phys. Chem.* 97 (1993) 4288.
- [31] D.G. Duff, P.P. Edwards, J. Evans, et al., *Angew. Chem. Intl. Edn.* 28 (1989) 590.
- [32] B. Moraweck, G. Clugnet, A.J. Renouprez, *Surf. Sci.* 81 (1979) 631.
- [33] P. Eisenberger, G.S. Brown, *Solid State Commun.* 29 (1979) 481.
- [34] L.B. Hansen, P. Stoltze, J.K. Nørskov, B.S. Clausen, W. Niemann, *Phys. Rev. Lett.* 64 (1990) 3155.
- [35] R.E. Benfield, *J. Chem. Soc. Faraday Trans.* 88 (1992) 1107.
- [36] B.S. Clausen, H. Topsøe, L.B. Hansen, P. Stoltze, J.K. Nørskov, *Jpn. J. Appl. Phys.* 32 (2) (1993) 95.
- [37] G. Meitzner, G.H. Via, F.W. Lytle, J.H. Sinfelt, *J. Phys. Chem.* 96 (1992) 4960.
- [38] S. Kruger, S. Vent, N. Rösch, *Ber. Bunsenges. Phys. Chem.* 101 (1997) 1640.
- [39] L.N. Lewis, N. Lewis, *J. Am. Chem. Soc.* 108 (1986) 7228.
- [40] G. Schmid, H. West, H. Mehles, A. Lehnert, *Inorg. Chem.* 36 (1997) 891.
- [41] J. Stein, L.N. Lewis, Y. Gao, R.A. Scott (submitted).